IOP PUBLISHING JOURNAL OF PHYSICS: CONDENSED MATTER

J. Phys.: Condens. Matter **20** (2008) 184008 (12pp) doi:10.1088/0953-8984/20/18/184008

Energy levels at interfaces between metals and conjugated organic molecules

Norbert Koch

Institut für Physik, Humboldt-Universität zu Berlin, Newtonstrasse 15, 12489 Berlin, Germany

E-mail: norbert.koch@physik.hu-berlin.de

Received 4 September 2007, in final form 27 October 2007
Published 17 April 2008
Online at stacks.iop.org/JPhysCM/20/184008

Abstract

The fundamental physical and chemical phenomena that can occur at interfaces between conjugated organic molecules and metal surfaces are discussed. The adsorption strength of molecular monolayers on metals covers a wide range from the weak physisorption regime to strong chemisorption, involving charge transfer and/or covalent bond formation. In many cases, molecular conformation changes can be observed, which directly impact the interface electronic structure and charge injection across the organic/metal contact. The energy level positions of organic multilayers are essentially determined by the monolayer/metal interaction, and 'flat-band' conditions prevail for thicker layers of pure organic molecules. Consequently, thermodynamic equilibrium across organic semiconductor films may not always be established.

(Some figures in this article are in colour only in the electronic version)

1. Introduction

The research on interfaces between metal surfaces and conjugated organic materials (COMs) is certainly driven by the interest in fundamental properties of such fascinating systems, i.e., the unique combination of 'hard' (metal) and 'soft' (organic) matter. Moreover, the huge success in realizing (opto-)electronic devices over the past 20 years has motivated many scientists to turn towards the field of organic/metal interfaces, and the number of active groups is still increasing today. Fully functional organic light emitting diodes (OLEDs) [1–8], field effect transistors (OFETs) [9–12], photovoltaic cells (OPVCs) [13–18], memory cells (OMCs) [19–21], and various sensing devices [22, 23] have been demonstrated, which are summarized by the term *organic electronics*. The benefits of using COMs (including small molecules and polymers) as alternatives to inorganic materials include their light weight, mechanical flexibility, and low cost thin film fabrication processes, i.e. simple high vacuum sublimation, spin-coating, inkjet-printing, transfer printing or even roll-to-roll printing. The wide tunability of COM electronic and structural properties *via* chemical synthesis is particularly attractive for this emerging technology, as the use of particular molecular moieties and/or combinations of COMs allows realizing defined insulating, semiconducting, or conducting materials. A common feature of all devices mentioned above is interfaces between semiconductor COMs and electrodes, across which charges have to be transported. Except for 'all-organic' devices, electrodes made of metals are commonly used. Consequently, the energy level alignment at the interface between the metal electrode and the organic semiconductor is of paramount importance for the injection of charges from the metal into the semiconductor, in analogy to the case of inorganic semiconductor/metal interfaces [24]. In *organic electronics*, thin film devices can be regarded as 'large area' entities, as typical lateral dimensions (depending on the specific application) cover the range from >10 cm to a few 100 nm. In contrast, the more recently emerged field of *molecular electronics* is dedicated to implementing functionality on the single or few molecular levels, which requires the understanding of contact properties on the molecular scale. In this case, the demands regarding experiment and theory are extremely stringent as 'every atom counts'. While single molecular electronic devices will not enter the market within the very near future, the progress of new knowledge on molecular scale contacts can readily help to understand also issues related to *organic electronics*. Therefore, the multidisciplinary nature of research in both fields will benefit from a strong mutual interaction of scientists.

In the context of *organic* and *molecular electronics* several key questions have to be answered to understand organic/metal interface (OMI) properties and their role in device function.

(i) What is the nature of the interaction between the COM and the metal?

(ii) How are energy levels aligned and distributed at the OMI due to a particular interaction?
(iii) How is charge injection and transport influenced by the interface energetics?

Experimentally, the most established tool to investigate interface electronic properties is photoelectron spectroscopy (PES). Because of its importance and wide use, the primary concepts of this technique will be laid out in the following. (Note that the use of PES for the investigation of organic/metal interfaces has been addressed in great detail before [25–28].) At first we consider the sample alone in vacuum (left part in figure 1(a)). Occupied electronic states are commonly divided into the valence region (VR) and core level (CL) region. The former contains electronic levels with a rather delocalized nature of the corresponding wavefunctions due to non-zero spatial overlap of the electron wavefunctions of the atoms constituting the solid. Such levels could be the valence bands of extended systems (covalent or van der Waals crystals, or polymers) or σ- and π-orbitals of molecules. The latter contains the localized atomic core levels that are shielded by valence electrons. At the surface of the sample a certain vacuum level (E_{vac}) exists, which is determined by both the sample's bulk *and* surface electronic structure and charge distribution. Together with the Fermi level (E_{F}), E_{vac} determines the sample work function (ϕ_{sample}) as indicated. E_{vac} is essentially constant in close proximity to the surface, but can vary significantly for differently terminated surfaces. In general, a surface has an inhomogeneous distribution of positive (atomic nuclei) and negative (electrons) charges along the surface normal, forming a surface dipole layer that contributes to E_{vac}. This, for instance, is the reason that different metal crystal faces exhibit different values of ϕ (e.g., for Cu, ϕ values of the (100), (110), and (111) surfaces spread over a range of about 0.5 eV [29, 30]). However, for distances r large compared to the lateral dimensions of the 2D surface dipole layer, its contribution to the electrostatic potential effectively reduces to that of a single dipole and E_{vac} decreases in proportion to r^{-2} [26] as shown in figure 1(a) for both sample and electron spectrometer. Consequently, at large distance from all surrounding matter the potential E_{vac} assumes a converged value, and an average work function ϕ_∞ could be defined.

In a PES experiment, the sample is irradiated with monochromatic electromagnetic radiation of energy $h\nu$ and photoelectrons are emitted. Commonly, vacuum ultraviolet radiation is used to measure VR (ultraviolet photoelectron spectroscopy—UPS) and x-rays have to be used to emit high binding energy CLs (x-ray photoelectron spectroscopy—XPS). Directly after emission the kinetic energy of the photoelectron is $E_{\mathrm{kin}} = h\nu - E_{\mathrm{B}} - \phi_{\mathrm{sample}}$ (figure 1(a)), where the electron binding energy E_{B} for a certain energy level is defined relative to E_{F}. The Fermi levels of the sample and the spectrometer are aligned in thermodynamic equilibrium. In most cases the work function of the spectrometer ϕ_{spec} will be different from ϕ_{sample}, and accordingly E_{vac} will show a variation along the electron trajectory as indicated in figure 1(a). However, the *measured* kinetic energy of the electron E'_{kin} is not influenced by the variation of E_{vac}, as only the *potential difference*

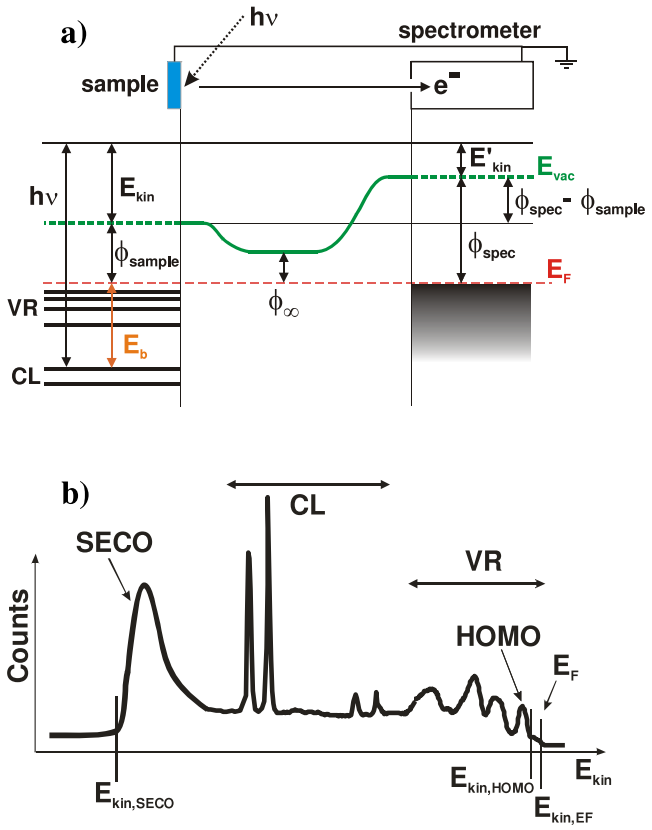

Figure 1. (a) Schematic energy level diagram for the sample and the electron spectrometer in a photoemission spectroscopy (PES) experiment. (b) Example for the various energy levels observed in an energy distribution curve (EDC) in a PES experiment. Please refer to the text for a detailed explanation.

between the sample surface and the spectrometer is relevant (as electrostatic interaction is conservative). Consequently, the following relation applies for E'_{kin}:

$$E'_{\mathrm{kin}} = h\nu - E_{\mathrm{B}} - \phi_{\mathrm{spec}} = E_{\mathrm{kin}} - (\phi_{\mathrm{spec}} - \phi_{\mathrm{sample}}). \quad (1)$$

For a given experimental set-up ϕ_{spec} is constant, and therefore E_{B} of electronic states of any sample can be measured, regardless of ϕ_{sample}. By keeping $h\nu$ fixed and sweeping the measured kinetic energy the energy distribution curve (EDC) is obtained, in its full range schematically depicted in figure 1(b). In addition to VR and CLs the secondary electron cut-off (SECO) at the lowest kinetic energy is shown. These secondary electrons stem from inelastically scattered (within the sample) photoelectrons, and electrons at the SECO's low energy cut-off were barely able to leave the sample in the limit of $E_{\mathrm{kin}} = 0$ eV. In a real experiment all electrons with $E_{\mathrm{kin}} < \phi_{\mathrm{spec}} - \phi_{\mathrm{sample}}$ would not be able to enter the spectrometer (cf figure 1(a)). In order to overcome this potential barrier and enable the measurement of the SECO, a negative potential of a few volts is applied to the sample, rigidly shifting all its energy levels upwards relative to the spectrometer (simply imagine this in figure 1(a)). Now the entire EDC is measured with a kinetic energy higher by the amount of the applied negative potential. From this measurement most parameters relevant in the context of organic/metal interfaces can be readily determined: the

sample work function ϕ_{sample}, the organic material's ionization energy IE, and the hole injection barrier HIB. The HIB is commonly defined as the energy difference between E_{F} and the low binding energy onset of the emission from the valence band or the highest occupied molecular orbital (HOMO). The corresponding relations according to figure 1(b) are

$$\begin{aligned} \phi_{\text{sample}} &= h\nu - \left(E_{\text{kin},EF} - E_{\text{kin,SECO}}\right) \\ \text{IE} &= h\nu - \left(E_{\text{kin,HOMO}} - E_{\text{kin,SECO}}\right) \\ \text{HIB} &= E_{\text{kin},EF} - E_{\text{kin,HOMO}}. \end{aligned} \tag{2}$$

In addition to the direct information from VR density of states, the exact binding energies of CLs provide valuable information on the chemical environment and bonding configuration of specific atom species. For all typical PES studies, it should be kept in mind that the kinetic energy of photoelectrons is in the range of some eV to several hundred eV, resulting in the high surface sensitivity of this technique, as the elastic mean free path of such electrons is below 1 nm [31]. Only recently, the advanced design of new electron spectrometers led to the development of high resolution 'high kinetic energy photoemission', with kinetic energies in excess of 10 keV, which extends the sensitivity of PES for bulk states significantly to over 10 nm [32–35]. In terms of lateral resolution, the use of spectroscopic photoemission electron microscopy (PEEM) has revealed that surface inhomogeneities on the length scale down to a few nanometers can have a tremendous impact on molecular layer growth and energetics [36–40]. The ultimate lateral resolution in studies on the electronic structure of adsorbates (i.e. intra-molecular length scale) can be achieved by scanning tunneling spectroscopy (STS) [41, 42], and the concomitant use of a scanned tip even allows the controlled manipulation of molecules on surfaces [43–45]. In contrast to PES, STS also allows probing of unoccupied states. Other methods to assess unoccupied states include inverse photoemission spectroscopy (IPES) [46–48] and two-photon photoemission spectroscopy [49, 50].

2. Monolayer formation

Over the past few years and after numerous detailed organic/metal interface studies it has transpired that the interaction between conjugated molecules and clean metal surfaces is a rather complex issue. Despite the huge number of systems that have been investigated, no universal picture has yet emerged, and one can conjecture that COM adsorption will remain a vividly debated field for many years to come. The possible types of interaction could be classified by physisorption (van der Waals) or chemisorption (possibly with a certain degree of charge transfer and/or covalent bond formation). A physisorbed molecule should retain its chemical integrity and orbital structure upon adsorption. If chemisorption occurs, the ordering of orbitals of the adsorbed molecule differs from that of the free (gas phase) molecule, due to hybridization with electron wavefunctions of the metal and/or a change in orbital population. Chemisorption can often

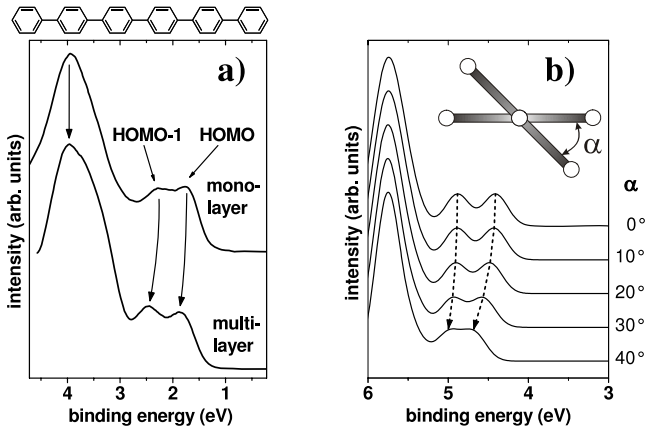

Figure 2. (a) Experimental UPS spectra for a *p*-sexiphenyl (6P) monolayer (top) and multilayer (bottom) on Ag(111). (b) Theoretical UPS spectra for a 6P molecule with various inter-ring twist angles α. The inset shows a view along the long axis of a 6P molecules defining α. Data are taken from [53].

readily be identified due to the appearance of new density of states (DOS) that is absent for both the free molecule and the clean metal (an example follows below). However, it is sometimes difficult to clearly differentiate between these two adsorption types if no clear new DOS can be observed, as will be shown by the following example.

A prototypical rod-like conjugated molecule is *p*-sexiphenyl (6P), which is an efficient blue light emitter in OLEDs [5]. UPS spectra of a 6P monolayer and multilayer on Ag(111) are shown as the top and bottom curves in figure 2(a), along with the molecule's chemical structure. It is known that 6P adsorbs with its long molecular axis parallel to the Ag(111) surface [51]. In order to allow for a direct comparison of DOS changes, the spectra have been shifted to align the strong photoemission peak at 3.9 eV binding energy, which is derived from the six almost degenerate lowest lying localized π-orbitals of 6P. The lowest binding energy maximum (at about 1.8 eV binding energy) is related to an ionization process of the highest occupied molecular orbital (HOMO), that at about 2.4 eV to the HOMO-1, both being delocalized π-orbitals [52]. Apparently, the HOMO and HOMO-1 are shifted 0.1 eV closer to the localized π-peak in the multilayer compared to the monolayer; i.e., the energy separation between localized and delocalized π-states is larger in the monolayer [53]. Except for this differential shift of molecular levels, no other changes were observed between the two spectra; most importantly, no new DOS (or intra-gap states [28, 54–57]) were found, ruling out strong chemisorptive bonding or charge transfer for 6P on Ag(111). This was supported by core level photoelectron spectroscopy of 6P on Ag(111), where no appearance of new C 1s peak components for monolayer coverage compared to multilayers was observed. Hence, the differential changes in molecular level binding energy must be due to differences in the molecular conformation of 6P between the monolayer and the thick film. At room temperature, 6P molecules in the bulk exhibit librational motion, resulting in angles between neighboring benzene ring planes (α, for definition see the

inset in figure 2(b), where the 6P molecule is viewed along its long molecular axis) different from zero. The short 6P analog biphenyl has an inter-ring twist angle of 42° in the gas phase [58] and 32° in solution and the molten state [59], whereas it was found to be planar on average [60] in the solid state as a result of ring librations at room temperature. However, for the longer *p*-quarterphenyl, an average twist of 22.7° between the two inner rings and 17.2° between the inner and outer rings in the low temperature phase was found [61], and slightly larger values were even estimated at room temperature [62]. As is very well established, larger α leads to smaller conjugation (inter-benzene π-electron overlap) along the 6P molecule, and consequently to a shift of energy levels and a larger energy gap [61]. Theoretical modeling using density functional theory (DFT) describes this behavior qualitatively [53] (see figure 2(b)). In particular, an increase of α leads to a decrease in the energy separation between the delocalized HOMO and the localized π-states, which are at about 5.7 eV below the vacuum level (as calculated by DFT; note that the binding energy scale in figure 2(a) is referred to E_F, thus no direct correspondence of the energy levels in figures 2(a) and (b) is provided; however, relative changes are relevant here) in figure 2(b) (and around 4 eV binding energy in figure 2(a)). The same trend was also observed experimentally (figure 2(a)). This observation is thus consistent with the fact that 6P molecules in direct contact with the Ag surface have a smaller inter-ring twist angle α than bulk 6P. This was also concluded by a scanning tunneling microscopy study on 6P/Ag(111) performed at 6 K, where $\alpha = 11.4°$ was reported [51]. From these observations and the crystallographic data discussed above, it can be deduced that the inter-ring twist angle in 6P at the Ag surface is reduced by about 10°. According to figure 2(b), this reduction of α is fully consistent with the 0.1 eV change in the binding energy difference observed experimentally between the delocalized and localized states [53]. This small, yet finite, interaction between the metal surface and 6P forces the molecule into a more coplanar conformation with increased π-electron overlap. Clearly, the energies of molecular states have been altered by adsorption compared to the molecule in the gas phase or in the bulk. However, there are no clear indications for chemisorption, as core level shifts or the formation of organic–metal hybrid states (intra-gap states) are lacking. Moreover, noticeable covalent molecule–metal bond formation was not observed in STM experiments, as the molecule could be moved around the Ag(111) surface by the tip without losing its integrity [51]. Finally, changes of α can simply be induced by van der Waals inter-molecular interactions, as discussed above for the various oligophenyls (e.g. α in the gas phase versus in the crystal). Therefore, the adsorption of 6P on Ag(111) could be classified as physisorptive. Here it is worth noting that COMs should not be considered as rigid entities: an adsorption, even a very weak one, can significantly change molecular conformation and thus the electronic properties of the molecule. Adsorption-induced molecular distortions are expected to be more pronounced for stronger molecule–metal interaction, which is, in fact, observed; examples for this phenomenon are, e.g., discussed in detail in the article by Kowarik *et al* [63], in this special issue.

Next, a model system will be discussed, which has been extensively investigated in the past, and thus deep understanding of the molecule–metal interaction is available: 3,4,9,10-perylene-tetracarboxylic acid dianhydride (PTCDA) on Ag(111). Very early it was observed that the UPS spectrum for monolayer PTCDA/Ag(111) differs significantly from the multilayer spectrum [64]. As the multilayer spectrum corresponds to neutral PTCDA molecules in the bulk, a strong chemical interaction between the Ag surface and the adsorbed monolayer was concluded [64]. A representative UPS spectrum for monolayer PTCDA/Ag(111) is shown as the bottom curve in figure 3(a), and it is very similar to those reported earlier [64, 65]. In contrast to the case of weakly adsorbed molecules, where no molecule-related DOS is observed in the binding energy region close to E_F (e.g., figure 2), here a significant photoemission intensity is observed that is absent for both clean metal surface and neutral multilayer spectra. These features are labeled H″ and L″ in figure 3(a), and their maxima have binding energies of about 1.6 and 0.3 eV, respectively. Zou *et al* [65] assigned these features as follows: PTCDA interacts strongly with the Ag surface involving significant charge transfer from the metal towards the molecule. Therefore, the LUMO of PTCDA becomes partially filled and thus shifts below E_F and is then detectable in UPS as feature L″ (which only probes occupied states). Most interestingly, a detailed shape analysis of L″ led to the conclusion that this molecular state is actually cut by E_F at room temperature, indicating only partial LUMO filling and a metallic molecular monolayer on Ag(111) [65]. Theoretical modeling yielded a transfer of approximately 0.6 electrons into the LUMO [66, 67]. The monolayer feature H″ was consequently assigned to be derived from the PTCDA HOMO, however modified due to the charge transfer into the LUMO. For multilayer PTCDA the HOMO is measured at 2.2 eV binding energy [65]. The transfer of negative charge into the adsorbed molecule may be expected to lead to a significant increase of the sample work function (on the order of 1 eV) due to the formation of a surface dipole with its negative end on the vacuum side [68, 69]. In contrast, the work function (ϕ) only increased by 0.1 eV upon adsorption of PTCDA on Ag(111) [65]. It was suggested that electron back-donation from the molecule to the metal occurs simultaneously, mostly involving the HOMO and HOMO-1 orbitals [65], which, however, seems to be at variance with calculations [66]. The actual dipole-induced ϕ change might actually be larger than 0.1 eV, as the counter-acting effect of metal electron 'push-back' due to molecular adsorption [26, 70–73] should be considered as well. Assuming as a common value for the 'push-back' a ϕ-reduction of 0.5 eV [74], the total dipole-related effective ϕ-increase for PTCDA/Ag(111) might be ∼0.6 eV. Note that this picture is probably over-simplified, as theoretical results point towards a relatively complex rearrangement of the charge distribution for this system [66]; and other theoretical investigations show that the charge density and potential distribution along the surface normal for strongly interacting organic/metal systems can be very rich in detail [71, 75, 76]. In summary, the schematic picture of the PTCDA/Ag(111) interface energetics as shown in figure 3(b)

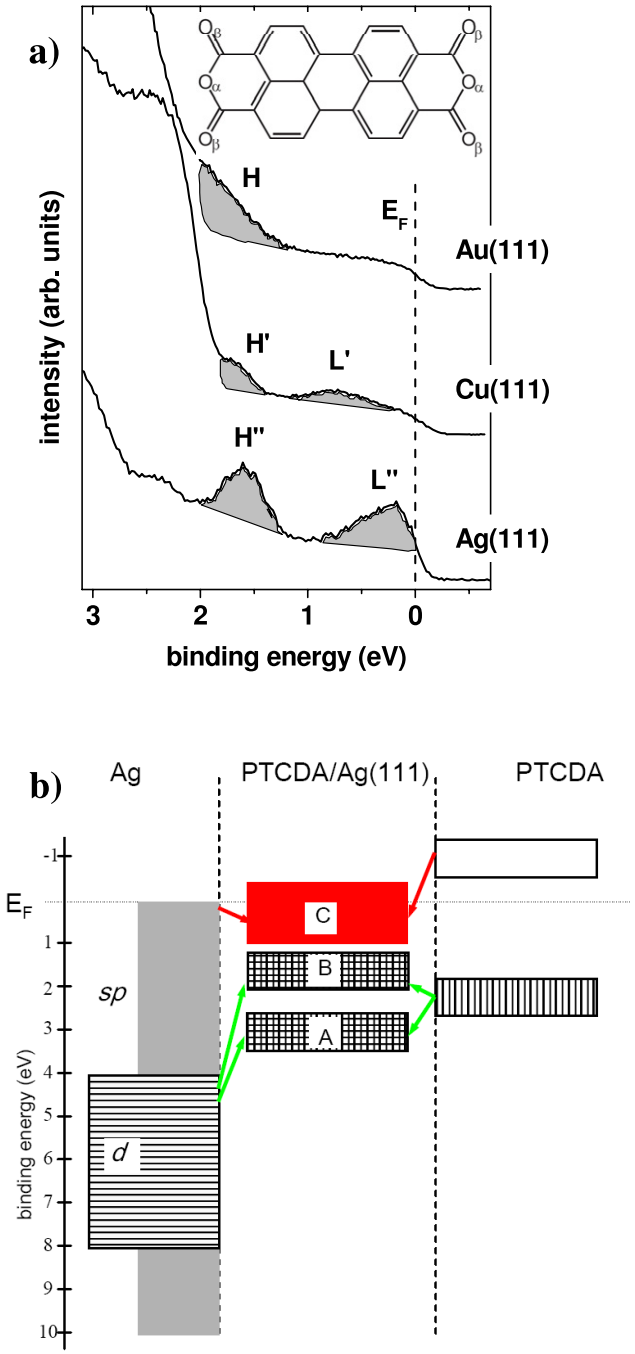

Figure 3. (a) UPS spectra of ca monolayer PTCDA on the metal surfaces as indicated. The peak labels are explained in the text. (b) Schematic energy level diagram for PTCDA/Ag(111) showing the hybridization of molecular and metal levels. 'A' corresponds to HOMO-2 of chemisorbed PTCDA, 'B' to the peak labeled H″, and the part of 'C' below E_F to the peak labeled L″ in part (a) of this figure. Part (b) is reprinted from Zou *et al* [65]. Copyright (2006) with permission from Elsevier.

was suggested [65], emphasizing the important point that pronounced hybridization of molecular and metal electron wavefunctions can occur for strongly chemisorbed systems.

In addition to the complex situation regarding energy levels of this interface, considerable *structural* changes were also reported for PTCDA on Ag(111). As the entire charge distribution on the molecule is altered due to adsorption, also the intra-molecular bond lengths and even bond angles change, as inferred from x-ray standing wave (XSW) experiments [66, 77]. As discussed in more detail in the contribution by Kowarik *et al* in this special issue [63], the planarity of neutral PTCDA is removed due to adsorption, with the anhydride oxygen atoms (labeled α in figure 3(a)) residing about 0.1 Å above the carbon backbone and the carboxylic oxygens (labeled β in figure 3(a)) about 0.2 Å below the average carbon plane, which itself is 2.86 Å above the Ag(111) surface [66]. This particular adsorption geometry is characteristic for the specific material pair. Replacing Ag(111) by Cu(111) results in pronounced changes regarding both adsorption geometry and interface electronic structure. The average carbon plane of PTCDA is significantly closer to the Cu(111) surface (2.66 Å), and both oxygen species reside above this plane (bonding distances of 2.89 Å for anhydride oxygen and 2.73 Å for carboxylic oxygen) [77]. These geometric changes have a profound impact on the molecular energy levels as apparent from the UPS spectrum of about monolayer PTCDA/Cu(111) (center curve in figure 3(a)). While the HOMO-derived level H′ is at a similar position compared to H″ (on Ag(111)), the LUMO-derived level L' is shifted completely below E_F, indicating that the PTCDA monolayer adsorbed in Cu(111) is semiconducting [78]. This observation is similar to that for PTCDA/Ag(110) [65], and might be related to a complete filling of the LUMO (which might be expected based on the observed smaller average molecule–metal bonding distance), as opposed to the partial filling on the Ag(111) surface, which yielded a metallic molecular monolayer (see above). However, details of the interfacial charge transfer balance may differ from this simple picture, as the peculiar adsorption geometry of PTCDA on Cu(111) could lead to differences in the hybridization of molecular and metal levels.

In contrast to the Ag and Cu substrates, no photoemission signature of a (partially) filled LUMO-derived molecular state could be found for PTCDA/Au(111) [78]. The corresponding monolayer spectrum (topmost curve in figure 3(a)) is flat between E_F and the onset of emission from the HOMO related feature (H). This absence of clear indications for charge transfer is fully consistent with the comparably large bonding distance found for PTCDA on Au(111) of 3.27 Å [79], which is close to the molecular stacking distance measured in PTCDA single crystals $d_{(102)} = 3.22$ Å [80]. Consequently, this interaction of PTCDA and Au(111) might be classified as physisorptive. However, theoretical considerations have emerged that involve the description of organic/metal interaction within a weak chemisorption framework and applying the density of interface states model [81, 82], originally developed for inorganic semiconductor/metal interfaces. This concept, first introduced by Vazquez *et al* [83], can be used to show that the proximity of the metal surface with a continuum of states broadens the molecular levels, e.g. with Lorentzian shape for weak interactions [84]. The broadening of molecular levels leads to a finite continuum of induced density of states in the

otherwise empty energy gap of the molecule. This induced DOS can be integrated up to the total charge of the isolated molecule, which then defines the position of the charge neutrality level (CNL). As all molecular levels are considered in this approach, and not just the HOMO and LUMO levels, the CNL will generally not be found at the mid-gap position. Finally, the relative positions of the CNL and the metal work function determine the direction and the amount of charge transferred across the interface [83, 84]. For the case of PTCDA/Au(111) the application of this model predicted that the induced DOS is large enough for a meaningful definition of the CNL, interestingly rather independent of the molecule–metal bonding distance. The theoretical work predicted that E_F at the interface should be close to the PTCDA CNL, which was placed ∼2.45 eV above the center of the HOMO [83]. From figure 3(a) it is difficult to determine the exact maximum of the photoemission feature associated with the PTCDA HOMO as it is superimposed by the intense emission from the Au substrate at binding energies > 2 eV. Provided that the emission from the HOMO might be broadened significantly, the peak maximum may indeed be above 2 eV. In fact, the HOMO maximum for multilayer PTCDA/Au(111) was found at 2.2 eV binding energy [78]. In the meantime, the CNL concept has been applied to a number of organic–metal systems [84], and even organic–organic heterojunctions [84, 85], providing strong indications for a predictive character of this model. Most importantly, it appears that other important interface effects can be accounted for in an extended CNL model. In addition to the broadening of molecular levels due to the metal proximity, metal–organic charge transfer and the 'push-back' effect can be included [86, 87], as well as intra-molecular and metal–organic bonding dipoles [88]. Such a unified CNL model, comprising all relevant contributions to the energy level alignment at organic/metal interfaces, could be generally applicable.

Once more, we turn back to PTCDA/Ag(111) to highlight yet another important aspect of organic/metal interfaces. As UPS is an area-averaging technique it is possible that subtle differences in interface energetics due to inequivalent molecular adsorption sites are not recognized. This issue has recently been exemplified by Kraft *et al* [89], who used scanning tunneling spectroscopy (STS) to reveal interface energy level differences for PTCDA/Ag(111) on the molecular scale. A detailed analysis of high resolution STM images revealed that the centers of all molecules are located at or close to bridge sites of the Ag surface. However, there exist two inequivalent molecular orientations; i.e., molecules of type A are almost perfectly aligned with the $[10\bar{1}]$ Ag lattice direction, while type B molecules are rotated by $(18 \pm 2)°$ with respect to $[0\bar{1}1]$ (cf figure 4). These subtle differences in adsorption geometry relative to the Ag substrate also lead to different and inequivalent inter-molecular interactions. The consequence can be seen in the STS curves recorded for A and B type molecules (figure 4(a)), where the resonances labeled L1 and L2 correspond to the states derived from the HOMO and LUMO of PTCDA (analogous states are labeled H″ and L″ in figure 3(a)). Apparently both levels are shifted relative to each other, the shift being larger for L2, which is mainly affected by the metal-to-molecule charge

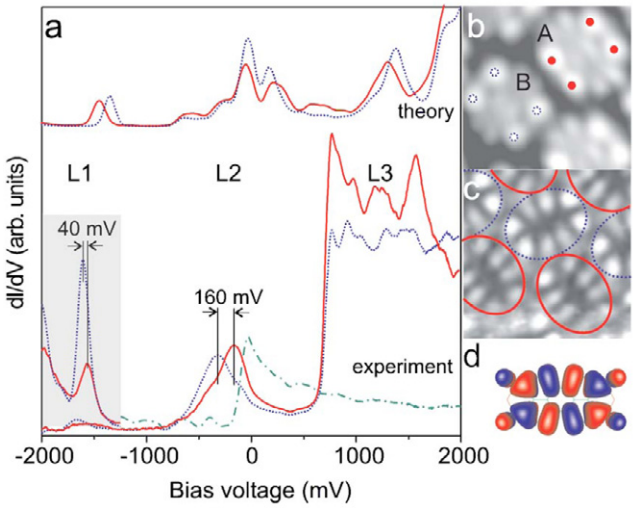

Figure 4. (a) Experimental background-subtracted and simulated dI/dV spectra for PTCDA/Ag(111), recorded on molecules of type A (red, full line) and B (blue, dotted line). Inequivalent PTCDA molecules are defined in the STM image (b). Green dash–dotted spectrum: Ag(111). (c) dI/dV image recorded in the left flank of L1. (d) Calculated free molecule HOMO. L2 corresponds to the peak labeled L″ in figure 3(a). Reproduced with permission from [89]. Copyright (2006) by the American Physical Society.

transfer [89]. The co-existence of these two slightly different bonding situations with their individual energy levels may then explain the highly asymmetric lineshape that was observed for L″ in UPS. We can thus expect that the concerted use of several experimental techniques, in particular those with very high lateral resolution, will reveal more fine details of the interaction between molecules and metal surfaces, which should enable a more reliable comparison of experiment to theory; this will lead to a significantly improved understanding of organic/metal interfaces.

The importance of understanding the fundamentals of adsorption behavior of molecules in the monolayer range becomes perceptible in the context of controlling the energy level alignment at organic/metal interfaces in devices. For instance, it has been shown that monolayers of molecules with strong electron accepting character can be used to adjust the energy level alignment at virtually any organic/metal interface. Strong acceptors, such as tetracyano-tetrafluoroquinodimethane (F4-TCNQ) [68] or octofluoroanthraquinone [90] chemisorb even on Au surfaces with noticeable charge transfer, leading to an increase of the surface ϕ. Any subsequently deposited COM aligns its energy levels relative to this new surface potential, and hole injection barriers (HIBs) are reduced accordingly [69]. For instance, it was shown that an F4-TCNQ monolayer on Au can reduce the HIB by up to 1.2 eV [68]. The development of new electron acceptors for this purpose can certainly benefit from a thorough knowledge of how molecules interact with metal surfaces, and how the delicate balance of adsorption-induced intra-molecular conformation changes and how charge rearrangement depends on the molecular structure.

3. Multilayer formation

Pentacene (PEN) is regarded as *the* prototypical COM; it is the most widely investigated organic system at present, and also is successfully used to fabricate OFETs with exceptionally high charge carrier mobility in excess of 5 $cm^2\ V^{-1}\ s^{-1}$ [11, 12]. Au is a widely used metal for contact formation in organic electronics. Therefore, the interface formed between PEN and Au(111) will be discussed in the following as a general example for multilayer formation [91]. The typical experimental approach using UPS is to start with the atomically clean metal surface, and then deposit increasing amounts of COM, making measurements after every step. Results from such a UPS experiment as a function of nominal coverage (θ) with PEN are shown in figure 5(a). It should be emphasized here that θ is a measure of the deposited mass rather than the true organic layer thickness, as—by and large—COMs rarely exhibit layer-by-layer growth on metal surfaces; very often Stranski–Krastanov or Volmer–Weber type growth prevails, as is also the case of PEN/Au, as will be detailed further below. Notably, the sample work function (ϕ) decreases from 5.50 eV (pristine Au) to 4.55 eV ($\theta \geqslant 4$ Å) upon adsorption of PEN, as inferred from the 0.95 eV shift of the secondary electron cut-off (SECO) towards lower kinetic energy (figure 5(b)). This change of the vacuum level (Δ_{vac}) has been attributed to the 'push-back' of metal surface electrons due to the presence of a weakly adsorbed organic layer [26, 70, 73]. In the wide scan view (figure 5(a)) the lowest binding energy emission feature observed after PEN deposition at about 1 eV is derived from the highest occupied molecular orbital (HOMO) of PEN. The binding energy region close to E_F and the HOMO is of particular interest when discussing interface energetics, and is thus shown in more detail in figure 5(c). For $\theta = 2$ Å (i.e. slightly less than a flat-lying PEN monolayer), the HOMO-derived narrow peak labeled '(1)' (centered at 0.90 eV) has its low binding energy onset at 0.70 eV below E_F; this value corresponds the HIB according to equation (2). Increasing θ (and thus partially covering the monolayer with further molecules to form multilayers) shifts this peak and its onset towards lower binding energy by 0.1 eV. The magnitude of this shift agrees well with the theoretically predicted increase of 130 meV in polarization energy for a PEN monolayer on Au upon adsorption of multilayers on top [92]. Thus the HIB of the monolayer is reduced to 0.60 eV. For $\theta \geqslant 8$ Å another peak (labeled '(2)') emerges, which increases in intensity for increasing coverage, while (1) decreases. This observation is consistent with the formation of PEN multilayers, as photoelectrons from the PEN monolayer (1) become attenuated by the molecules adsorbed on top to form multilayers. Island growth of PEN on Au is well documented in the literature [93–95], and fully supported by the observation of intensity from the substrate metal E_F even at $\theta = 110$ Å, which is significantly larger than the elastic mean free path of the photoelectrons. Consequently, feature (2) is related to the HOMO-derived emission of PEN in the multilayer. The peak center is at about 1.2 eV binding energy. The low binding energy onset can, however, not be determined reliably, since emission from (1) is superimposed on that from (2) (island growth) in all spectra. Assuming a similar width of peaks (1) and (2), the HIB for multilayers is estimated to be about 0.9 eV. Note that the shift of about 0.3 eV to higher binding energy when going from monolayer to multilayer affects all valence levels by the same amount (rigid shift), as well as the C 1s core levels (not shown). Conversely, the position of the SECO does not change between mono- and multilayer coverage. The shift of electronic levels is thus not due to changes in molecular conformation (which would require differential shifts) or surface potential, but it is of electrostatic nature.

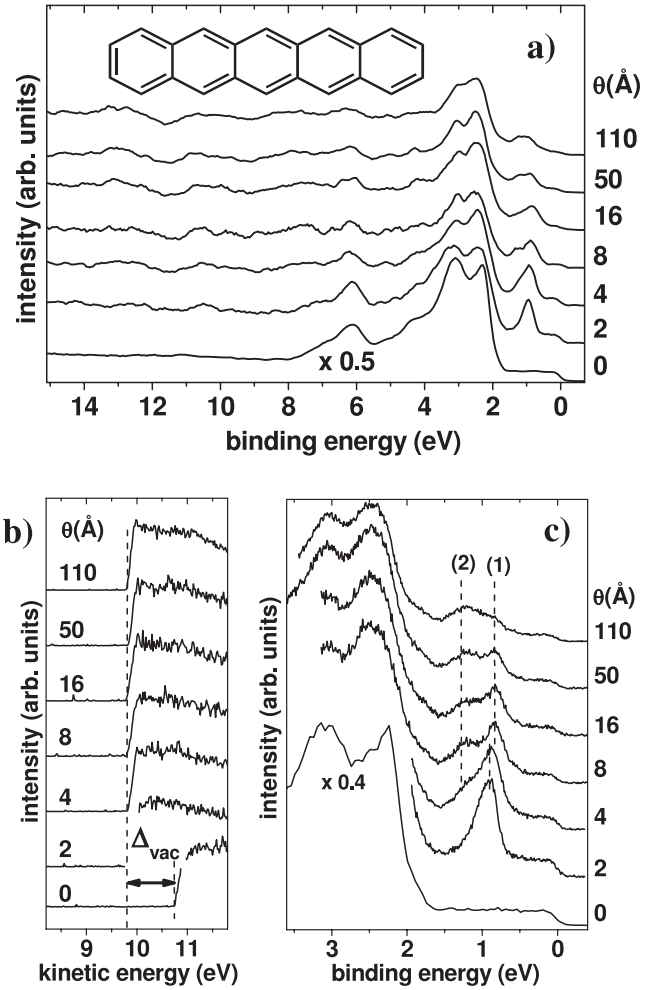

Figure 5. UPS spectra of pentacene (PEN) deposited onto Au(111) for increasing coverage θ. (a) Survey valence region spectra. (b) Secondary electron cut-off (SECO), and (c) near-E_F low binding energy region. (1) Corresponds to emission from the PEN monolayer HOMO, (2) to the PEN HOMO of multilayers.

The kinetic energy of photoelectrons and thus the measured ionization energy (IE) is affected by a polarization of the photohole's surroundings. The sudden presence of the hole left behind by the photoionization process leads to a very fast (fs timescale) polarization of all surrounding matter, thus 'screening' the Coulomb attraction between the photoelectron and its hole. More efficient screening results in higher kinetic energy (=lower binding energy). The position of the SECO is not affected by screening, as these electrons with $E_{kin} = 0$ eV have no defined initial state (they were inelastically scattered).

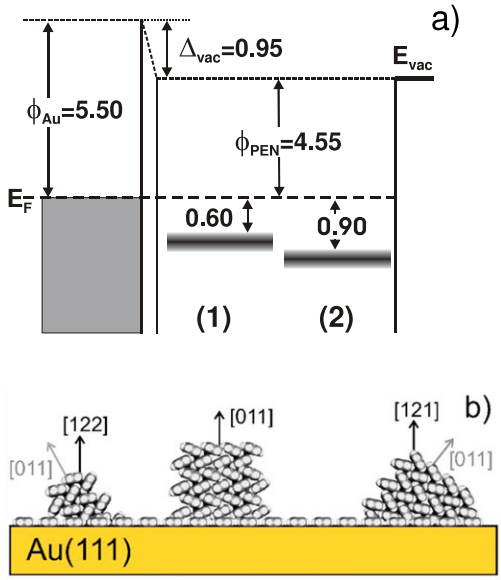

Figure 6. (a) Schematic energy level diagram of the PEN/Au(111) interface (for details see the text). (1) is for the PEN monolayer, (2) for the multilayer. (b) Representation of the PEN morphology and molecular orientation on Au(111). Part (b) is reproduced with permission from [95]. Copyright (2007) by the American Physical Society.

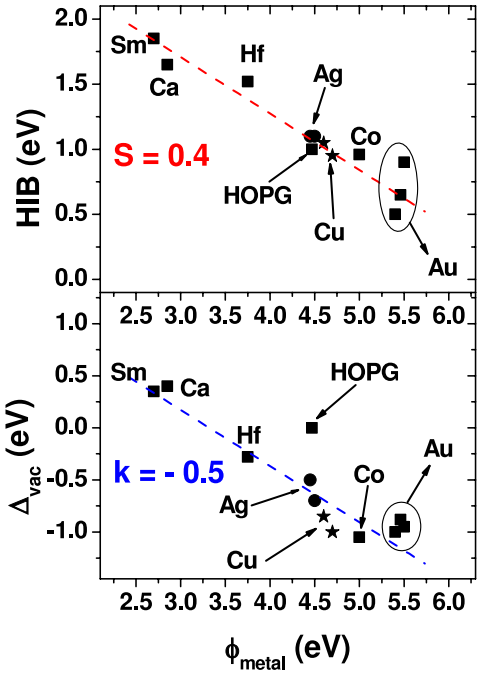

Figure 7. Hole injection barrier (HIB) and vacuum level shift (Δ_{vac}) for pentacene on various metals as a function of the pristine metal surface work function ϕ_{metal}. The lines are linear fits to the data (the point for HOPG in the lower part was excluded from fitting).

For COM thin films on metals, screening is due to (i) the metal substrate and (ii) the surrounding molecules. Photo-hole screening by the metal substrate has been identified for various organic molecules on a range of substrates [26, 27, 53, 96]. With increasing thickness of the organic layer the screening by the metal becomes less efficient, resulting in an apparent shift of all molecular levels to higher binding energy with respect to both E_F and E_{vac}, and thus an increase in the measured IE. Typically, the magnitude of this shift is found to be in the range of 0.2–0.4 eV [53, 96], depending on the specific system under investigation. For the present case of PEN/Au(111), the total change in polarization energy between the monolayer PEN on Au(111) not covered by multilayers and the surface of the thick PEN film is about 0.4 eV, in reasonable agreement with calculations, that gave about 360 meV for this value [26, 27, 92]. This energetic situation of the PEN/Au(111) interface is summarized in figure 6(a).

As the relative emission intensities of (1) and (2) are markedly different in figure 5(c), it can be proposed that PEN multilayers do not exhibit a flat-lying adsorption geometry (molecular plane parallel to the surface). However, molecules in the multilayer do not exhibit a 'standing-upright-like' geometry (as on SiO_2 [97]). Most likely, PEN in multilayers adopts a herringbone arrangement similar to its crystal bulk. In fact, a recent x-ray diffraction and near-edge x-ray absorption study by Käfer *et al* [95] showed that the growth of PEN on atomically clean Au(111) is indeed characterized by a flat-lying monolayer and multilayer islands, whose (011), (121), and (122) faces are parallel to the Au(111) surface [95], as schematically shown in figure 6(b). Note that if the Au surface is polycrystalline or modified by other organic molecules (including contamination from ambient air exposure) the orientation of PEN can differ markedly [95], and also the interface energy level alignment is strongly affected [69, 98].

For various applications it is necessary to use contacts other than Au, and thus many studies were reported for PEN deposited on various metal substrates, covering a wide range of work function and chemical reactivity. Plotting the key parameters of PEN/metal interfaces (i.e., hole injection barrier and vacuum level shift) as a function of substrate ϕ_{metal} results in figure 7. While there is some scatter of data points for the HIB (in particular for Au, possibly due to varying orientation of molecules on the respective surfaces [74, 95]), there still seems to be a linear relationship between metal ϕ and the magnitude of the HIB. A linear fit through all points yields the 'slope-parameter' $S = 0.4$ [27], defined as $S = \frac{\mathrm{dHIB}}{\mathrm{d}\phi_{metal}}$. This value is between those expected for the Schottky–Mott limit ($S = 1$) and strict Fermi level pinning ($S = 0$) [27, 69, 99, 100]. Consequently, the finite interaction of PEN with these metal surfaces leads to a behavior that may be described using the charge neutrality level (CNL) model [84]. It should be interesting to see in the future if this model is applicable throughout the wide range of interaction strengths prevailing at the individual interfaces: strong chemisorption of PEN on Co [101], Cu [102] and Ca [103] was reported, whereas the interaction with the other metals was found to be significantly weaker (Sm [104], Hf [105], Ag [74, 103], HOPG [106, 107], Au [91, 103, 108]). The fact that $S \neq 1$ implies that interface dipoles Δ_{vac} (i.e. changes of ϕ between the clean metal surface and that covered with molecules) are required at these interfaces, which indeed was observed (figure 7(b)). A slope $k = \frac{\mathrm{d}\Delta_{vac}}{\mathrm{d}\phi_{metal}} = -0.5$ fits best to these data (the value for HOPG was excluded from the fit as it is not strictly a metal,

with electrons spilling into vacuum forming a surface dipole). The full consistency of HIB and Δ_{vac} values for all metal surfaces would require $S + k = 0$, which is almost fulfilled, as this sum is -0.1 for PEN. In general, S-values for organic molecules on metal surfaces span a wide range. S-parameters similar to that of PEN have been found for N,N'-bis-(1-naphthyl)-N,N'-diphenyl1-1,1-biphenyl1-4,4′-diamine (α-NPD: 0.5), 4,4′-N,N'-dicarbazole-biphenyl (CBP: 0.6) [27] and *para*-sexiphenyl (6P: 0.5) [109]. The largest value of S for an organic molecule on metal surfaces has been reported for aluminum tris(8-hydroxyquinoline) (Alq3: 0.8) [27], but no values close to $S = 1$ have occurred yet. In contrast, $S \approx 0$ has been obtained for several molecules (3,4,9,10-perylene-tetracarboxylic acid dianhydride—PTCDA; 3,4,9,10-perylenetetracarboxylic bisbenzimidazole—PTCBI; perfluorinated Cu phthalocyanine—F_{16}CuPc) [27]. It has been suggested that the magnitude of S correlates with the metal-induced density of states within the energy gap of the adsorbed molecule and the relative weight of occupied and unoccupied densities of states of frontier orbitals [86]. In comparison, it is interesting to note that interfaces between COMs and electrodes made of non-metals, in particular including oxides and conducting polymers, are characterized by a value of S very close to 1, meaning that the Schottky–Mott-limit is almost reached [69, 99, 100, 109]. However, for every specific COM there exist critical (non-metal) substrate ϕ-values where a transition to Fermi level pinning behavior occurs [69, 99].

One more issue is worth pointing out for COM multilayer energetics at interfaces to metals: thermodynamic equilibrium may not be established across the organic layer. As can be seen from figure 2, a certain vacuum level (electrostatic potential) is established after the adsorption of the first layer, and no further changes in E_{vac} occur upon multilayer formation. This is due to the fact that layers on top of the monolayer are bound by weak van der Waals inter-molecular forces, implying vacuum level alignment between molecular layers. The same phenomenon holds for the electronic levels. Apart from changes in the monolayer due to organic/metal interaction, and the above discussed photoelectron screening shifts (which saturate after a few nanometers) no binding energy shifts as a function of organic film thickness are observed. These 'flat-band' conditions are commonly observed for the vast majority of organic/metal interfaces. Note that UPS can only be applied for COM thicknesses up to a few 10 nm as charging becomes problematic for larger thickness [110, 111]. Device-relevant thickness ranges (a few hundred nanometers or more) can be investigated with the Kelvin-probe (KP) method, as exemplified in figure 8 [112]. This example shows nicely that no vacuum level shifts for the COM N,N'-bis(3-methylphenyl)-N,N'-diphenyl-[1,1′-biphenyl]-4,4′-diamine (TPD) are observed for thicknesses >100 nm, regardless of the metal substrate used. In contrast, 'band-bending', i.e. changes of the DOS binding energy with respect to E_F as function of distance from the interface, is often found for interfaces between inorganic semiconductor materials and metals [24]. Band-bending is due to charge accumulation/depletion in the semiconductor in the near-interface region or due to (charged) chemical impurities,

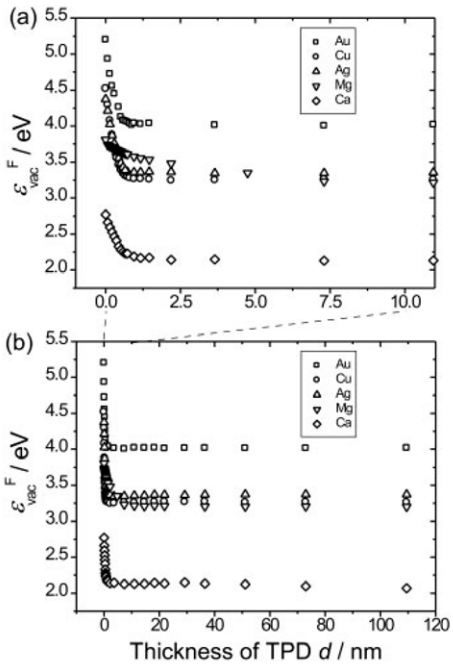

Figure 8. Variation of the vacuum level relative to the Fermi level ε_{vac}^{F} (corresponds to the sample work function) for TPD on Au, Cu, Ag, Mg and Ca substrates as a function of TPD thickness d. (a) The region for small d up to 10 nm is expanded. (b) The whole region up to $d = 110$ nm. Reproduced with permission from [112]. Copyright by Wiley-VCH Verlag GmbH & Co. KGaA.

rendering it an electrostatic effect due to space charges that shift E_{vac} and the DOS in one direction by the same amount. Therefore, effects such as molecular level energy changes due to organic/metal chemisorption, molecular conformation changes, screening, or energy band *dispersion* [113–117] should not be included in the use of the term band- or energy level bending. The reasons for the generally observed flat-band conditions at organic/metal interfaces for device-relevant thickness ranges are the high purity of the COMs and their comparably wide energy gap (i.e. very low concentration of thermally activated mobile charge carriers) [112]. If charged impurities are included in the COM, or intentional doping is introduced, band-bending can actually be observed for COMs, e.g. as was shown for C_{60} with a very wide space charge layer of ∼500 nm for an effective charged impurity (doping) concentration in the ppm range [112]. Consequently, for very pure organic materials, the Fermi level of the substrate and the one in the organic layer are not aligned, as for instance in figure 8 the substrate E_F is found at rather different positions in the TPD energy gap for different substrate metals.

As it is impossible to directly assess the (local) position of E_F in the gap of an organic thin film, other means have to be used to visualize the possible lack of thermodynamic equilibrium between metal contacts and COM thicker films. This can be done in a UPS experiment by depositing a metal M, which is very different from the substrate metal, on top of a closed (i.e. pin-hole free) organic layer. In practice, a high ϕ substrate in combination with a low ϕ top M can yield the desired effect. This structure can be regarded as two metal

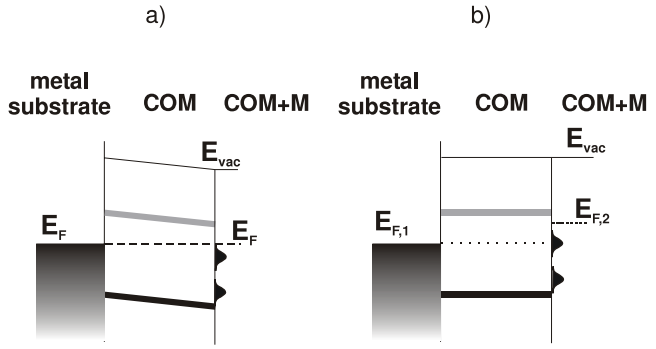

Figure 9. Schematic energy level diagram for an organic film (COM) on a metallic substrate, showing the HOMO (black bar), the LUMO (gray bar), and top metal (M) gap states on the surface: (a) in thermodynamic equilibrium and (b) in non-equilibrium. E_{vac} indicates the position of the vacuum level. In (a) the dashed line represents the position of E_{F} throughout the whole sample in thermodynamic equilibrium. In (b), the dotted line represents the position of the Fermi level $E_{\mathrm{F},1}$ of the metal substrate, and $E_{\mathrm{F},2}$ the local Fermi level on the surface.

contacts with different ϕ-values on opposite sides of the COM layer, as depicted in figure 9. In thermodynamic equilibrium, the Fermi levels of the two metals line up and a built-in voltage (the difference of the two metal ϕ-values) drops across the organic layer (figure 9(a)); possible band-bending effects in the COM layer are neglected in this example. However, several experiments have yielded an energetic situation according to figure 9(b); i.e., the Fermi level of the substrate $E_{\mathrm{F},1}$ and that of the top metal layer $E_{\mathrm{F},2}$ were not aligned, and occupied DOS of the top layer was observed *above* $E_{\mathrm{F},1}$, clearly indicating non-equilibrium conditions [57, 118–120]. Consequently, care has to be taken when evaluating UPS data of metal deposits on COM films, as the alignment of Fermi levels at opposite sides of an organic layer may not be established.

4. Conclusions

While for some organic/metal systems (a few of them were discussed here) a sound understanding of interfacial phenomena already exists, a generally applicable picture for this important class of interfaces is still lacking. The complex interplay of molecular adsorption-induced charge redistribution and concomitant conformation changes of molecules determines the energy level alignment at organic/metal interfaces and the efficiency and dynamics of charge transport across the contact. Therefore, we should hope to have refined experimental and theoretical tools at hand in the future to advance our comprehension of interface physico-chemical processes. Improved knowledge in the field will help to find rational approaches for controlling interface properties via the use of tailored molecules. This will facilitate exciting new developments in *organic* and *molecular electronics*.

Acknowledgment

The author would like to thank Steffen Duhm, Ingo Salzmann and Professor Jürgen P Rabe (HU-Berlin), Dr Antje Vollmer (BESSY), Professor Antoine Kahn and Professor Jeffrey Schwartz (Princeton University) and Professor Egbert Zojer (TU-Graz) for vital and stimulating discussions. Financial support was provided by the DFG (Sfb448 and Emmy Noether-Program), H C Starck GmbH & Co. KG, and the EC (project 'ICONTROL'; EC-STREP-033197).

References

[1] Burroughes J H, Bradley D D C, Brown A R, Marks R N, Mackey K, Friend R H, Burns P L and Holmes A B 1990 *Nature* **347** 539
[2] Baldo M A, O'Brien D F, You Y, Shoustikov A, Sibley S, Thompson M E and Forrest S R 1998 *Nature* **395** 151
[3] Schwartz G, Fehse K, Pfeiffer M, Walzer K and Leo K 2006 *Appl. Phys. Lett.* **89** 083509
[4] Pfeiffer M, Forrest S R, Leo K and Thompson M E 2002 *Adv. Mater.* **14** 1633
[5] Tasch S, Brandstatter C, Meghdadi F, Leising G, Froyer G and Athouel L 1997 *Adv. Mater.* **9** 33
[6] Scherf U and List E J W 2002 *Adv. Mater.* **14** 477
[7] Piok T *et al* 2003 *Adv. Mater.* **15** 800
[8] Pogantsch A, Rentenberger S, Langer G, Keplinger J, Kern W and Zojer E 2005 *Adv. Funct. Mater.* **15** 403
[9] Dimitrakopoulos C D and Malenfant P R L 2002 *Adv. Mater.* **14** 99
[10] Jurchescu O D, Baas J and Palstra T T M 2004 *Appl. Phys. Lett.* **84** 3061
[11] Kelley T W, Baude P F, Gerlach C, Ender D E, Muyres D, Haase M A, Vogel D E and Theiss S D 2004 *Chem. Mater.* **16** 4413
[12] Lee S, Koo B, Shin J, Lee E, Park H and Kim H 2006 *Appl. Phys. Lett.* **88** 162109
[13] Peumans P, Uchida S and Forrest S R 2003 *Nature* **425** 158
[14] Granström M, Petritsch K, Arias A C, Lux A, Andersson M R and Friend R H 1998 *Nature* **395** 257
[15] Li G, Shrotriya V, Huang J S, Yao Y, Moriarty T, Emery K and Yang Y 2005 *Nat. Mater.* **4** 864
[16] Hoppe H and Sariciftci N S 2006 *J. Mater. Chem.* **16** 45
[17] Ma W, Yang C, Gong X, Lee K and Heeger A J 2005 *Adv. Funct. Mater.* **15** 1617
[18] Schmidt-Mende L, Fechtenkötter A, Müllen K, Moons E, Friend R H and MacKenzie J D 2001 *Science* **293** 1119
[19] Ma L P, Liu J and Yang Y 2002 *Appl. Phys. Lett.* **80** 2997
[20] Yang Y, Ouyang J, Ma L P, Tseng R J H and Chu C W 2006 *Adv. Funct. Mater.* **16** 1001
[21] Scott J C and Bozano L D 2007 *Adv. Mater.* **19** 1452
[22] Loi A, Manunza I and Bonfiglio A 2005 *Appl. Phys. Lett.* **86** 103512
[23] Savvate'ev V *et al* 2002 *Appl. Phys. Lett.* **81** 4652
[24] Sze S Z 1981 *Physics of Semiconductor Devices* 2nd edn (New York: Wiley)
[25] Cahen D and Kahn A 2003 *Adv. Mater.* **15** 271
[26] Ishii H, Sugiyama K, Ito E and Seki K 1999 *Adv. Mater.* **11** 605
[27] Kahn A, Koch N and Gao W Y 2003 *J. Polym. Sci.* B **41** 2529
[28] Salaneck W R, Friend R H and Bredas J L 1999 *Phys. Rep.* **319** 231
[29] Michaelson H B 1977 *J. Appl. Phys.* **48** 4729
[30] Skriver H L and Rosengaard N M 1992 *Phys. Rev.* B **46** 7157
[31] Hüfner S 1995 *Photoelectron Spectroscopy* (Berlin: Springer)
[32] Kobayashi K *et al* 2003 *Appl. Phys. Lett.* **83** 1005
[33] Thiess S, Kunz C, Cowie B C C, Lee T L, Renier M and Zegenhagen J 2004 *Solid State Commun.* **132** 589
[34] Panaccione G *et al* 2005 *J. Phys.: Condens. Matter* **17** 2671
[35] Fecher G, Balke B, Ouardi S, Felser C, Schönhense G, Ikenaga E, Kim J J, Ueda S and Kobayashi K 2007 *J. Phys. D: Appl. Phys.* **40** 1576

[36] Yasufuku H, Ibe T, Okumura M, Kera S, Okudaira K K, Harada Y and Ueno N 2001 *J. Appl. Phys.* **90** 213
[37] Schmidt T, Groh U, Fink R and Umbach E 2002 *Surf. Rev. Lett.* **9** 223
[38] Hu W S, Tao Y T, Hsu Y J, Wei D H and Wu Y S 2005 *Langmuir* **21** 2260
[39] Shionoiri M, Yamamoto I, Onoue M, Kera S, Okudaira K K and Ueno N 2005 *Synth. Met.* **152** 301
[40] Marchetto H, Groh U, Schmidt T, Fink R, Freund H J and Umbach E 2006 *Chem. Phys.* **325** 178
[41] Jäckel F, Watson M D, Müllen K and Rabe J P 2004 *Phys. Rev. Lett.* **92** 188303
[42] Iancu V and Hla S-W 2006 *Proc. Natl Acad. Sci.* **103** 13718
[43] Hla S-W, Bartels L, Meyer G and Rieder K H 2000 *Phys. Rev. Lett.* **85** 2777
[44] Hecht S 2003 *Angew. Chem. Int. Edn* **42** 24
[45] Samori P 2004 *J. Mater. Chem.* **14** 1353
[46] Sato N, Yoshida H and Tsutsumi K 2000 *J. Mater. Chem.* **10** 85
[47] Hill I G, Kahn A, Soos Z G and Pascal R A 2000 *Chem. Phys. Lett.* **327** 181
[48] Zahn D R T, Gavrila G N and Salvan G 2007 *Chem. Rev.* **107** 1161
[49] Zhu X Y 2004 *J. Phys. Chem.* B **108** 8778
[50] Kirchmann P S, Loukakos P A, Bovensiepen U and Wolf M 2005 *New J. Phys.* **7** 113
[51] Braun K-F and Hla S-W 2005 *Nano Lett.* **5** 73
[52] Seki K, Karlsson U O, Engelhardt R, Koch E E and Schmidt W 1984 *Chem. Phys.* **91** 459
[53] Koch N, Heimel G, Wu J, Zojer E, Johnson R L, Brédas J-L, Müllen K and Rabe J P 2005 *Chem. Phys. Lett.* **413** 390
[54] Ramsey M G, Steinmuller D and Netzer F P 1990 *Phys. Rev.* B **42** 5902
[55] Hirose Y, Kahn A, Aristov V, Soukiassian P, Bulovic V and Forrest S R 1996 *Phys. Rev.* B **54** 13748
[56] Shen C F, Hill I G and Kahn A 1999 *Adv. Mater.* **11** 1523
[57] Koch N, Rajagopal A, Ghijsen J, Johnson R L, Leising G and Pireaux J J 2000 *J. Phys. Chem.* B **104** 1434
[58] Almenningen A, Bastiansen O, Fernholt L, Cyvin B, Cyvin S and Samdal S 1985 *J. Mol. Struct.* **128** 59
[59] Eaton V J and Steele D 1973 *J. Chem. Soc. Faraday Trans.* **2** 1601
[60] Trotter B 1961 *Acta Crystallogr.* **14** 1135
[61] Baudour J L, Délugeard Y and Rivet P 1978 *Acta Crystallogr.* B **34** 625
[62] Baudour J L 1991 *Acta Crystallogr.* B **47** 935
[63] Kowarik S, Gerlach A and Schreiber F 2008 *J. Phys.: Condens. Matter* **20** 184005
[64] Jung M, Baston U, Schnitzler G, Kaiser M, Papst J, Porwol T, Freund H J and Umbach E 1993 *J. Mol. Struct.* **293** 239
[65] Zou Y, Kilian L, Schöll A, Schmidt T, Fink R and Umbach E 2006 *Surf. Sci.* **600** 1240
[66] Hauschild A, Karki K, Cowie B C C, Rohlfing M, Tautz F S and Sokolowski M 2005 *Phys. Rev. Lett.* **94** 036106
[67] Hauschild A, Karki K, Cowie B C C, Rohlfing M, Tautz F S and Sokolowski M 2005 *Phys. Rev. Lett.* **95** 209602
[68] Koch N, Duhm S, Rabe J P, Vollmer A and Johnson R L 2005 *Phys. Rev. Lett.* **95** 237601
[69] Koch N 2007 *ChemPhysChem* **8** 1483
[70] Bagus P S, Staemmler V and Wöll C 2002 *Phys. Rev. Lett.* **89** 096104
[71] Bagus P S, Hermann K and Wöll C 2005 *J. Chem. Phys.* **123** 184109
[72] Witte G, Lukas S, Bagus P S and Wöll C 2005 *Appl. Phys. Lett.* **87** 263502
[73] Koch N, Ghijsen J, Pireaux J-J, Schwartz J, Johnson R L, Elschner A and Kahn A 2003 *Appl. Phys. Lett.* **82** 70
[74] Koch N, Salzmann I, Johnson R L, Pflaum J, Friedlein R and Rabe J P 2006 *Org. Electron.* **7** 537
[75] Crispin X, Geskin V, Crispin A, Cornil J, Lazzaroni R, Salaneck W R and Bredas J L 2002 *J. Am. Chem. Soc.* **124** 8131
[76] Heimel G, Romaner L, Bredas J L and Zojer E 2006 *Phys. Rev. Lett.* **96** 196806
[77] Gerlach A, Sellner S, Schreiber F, Koch N and Zegenhagen J 2007 *Phys. Rev.* B **75** 045401
[78] Duhm S, Gerlach A, Salzmann I, Bröker B, Johnson R L, Schreiber F and Koch N 2007 *Org. Electron.* at press doi:10.1016/j.orgel.2007.10.004
[79] Henze S K M, Bauer O, Lee T L, Sokolowski M and Tautz F S 2007 *Surf. Sci.* **601** 1566
[80] Möbus M, Karl N and Kobayashi T 1992 *J. Cryst. Growth* **116** 495
[81] Flores F and Tejedor C 1987 *J. Phys. C: Solid State Phys.* **20** 145
[82] Mönch W 1994 *Surf. Sci.* **299** 928
[83] Vazquez H, Oszwaldowski R, Pou P, Ortega J, Perez R, Flores F and Kahn A 2004 *Europhys. Lett.* **65** 802
[84] Vazquez H, Flores F and Kahn A 2007 *Org. Electron.* **8** 241
[85] Kahn A, Zhao W, Gao W, Vazquez H and Flores F 2006 *Chem. Phys.* **325** 129
[86] Vazquez H, Flores F, Oszwaldowski R, Ortega J, Perez R and Kahn A 2004 *Appl. Surf. Sci.* **234** 107
[87] Vazquez H, Dappe Y J, Ortega J and Flores F 2007 *J. Chem. Phys.* **126** 144703
[88] Vazquez H 2007 private communication
[89] Kraft A, Temirov R, Henze S K M, Soubatch S, Rohlfing M and Tautz F S 2006 *Phys. Rev.* B **74** 041402(R)
[90] Duhm S, Glowatzki H, Cimpeanu V, Klankermayer J, Rabe J P, Johnson R L and Koch N 2006 *J. Phys. Chem.* B **110** 21069
[91] Koch N, Vollmer A, Duhm S, Sakamoto Y and Suzuki T 2007 *Adv. Mater.* **19** 112
[92] Tsiper E V and Soos Z G 2003 *Phys. Rev.* B **68** 085301
[93] Koch N, Elschner A, Schwartz J and Kahn A 2003 *Appl. Phys. Lett.* **82** 2281
[94] Beernink G, Strunskus T, Witte G and Wöll C 2004 *Appl. Phys. Lett.* **85** 398
[95] Käfer D, Ruppel L and Witte G 2007 *Phys. Rev.* B **75** 085309
[96] Hill I G, Makinen A J and Kafafi Z H 2000 *J. Appl. Phys.* **88** 889
[97] Ruiz R, Nickel B, Koch N, Feldman L C, Haglund R F, Kahn A and Scoles G 2003 *Phys. Rev.* B **67** 125406
[98] Rentenberger S, Vollmer A, Schennach R, Zojer E and Koch N 2006 *J. Appl. Phys.* **100** 053701
[99] Crispin A, Crispin X, Fahlman M, Berggren M and Salaneck W R 2006 *Appl. Phys. Lett.* **89** 213503
[100] Tengstedt C, Osikowicz W, Salaneck W R, Parker I D, Hsu C H and Fahlman M 2006 *Appl. Phys. Lett.* **88** 053502
[101] Tiba M V, de Jonge W J M, Koopmans B and Jonkman H T 2006 *J. Appl. Phys.* **100** 093707
[102] McDonald O, Cafolla A A, Li Z and Hughes G 2006 *Surf. Sci.* **600** 1909
[103] Watkins N J, Yan L and Gao Y 2002 *Appl. Phys. Lett.* **80** 4384
[104] Koch N, Ghijsen J, Johnson R L, Schwartz J, Pireaux J-J and Kahn A 2002 *J. Phys. Chem.* B **106** 4192
[105] Kang S J, Yi Y J, Kim C Y and Whang C N 2005 *J. Korean Phys. Soc.* **46** L760
[106] Fukagawa H, Yamane H, Kataoka T, Kera S, Nakamura M, Kudo K and Ueno N 2006 *Phys. Rev.* B **73** 245310
[107] Yamane H, Nagamatsu S, Fukagawa H, Kera S, Friedlein R, Okudaira K K and Ueno N 2005 *Phys. Rev.* B **72** 153412
[108] McDonald O, Cafolla A A, Carty D, Sheerin G and Hughes G 2006 *Surf. Sci.* **600** 3217
[109] Koch N and Vollmer A 2006 *Appl. Phys. Lett.* **89** 162107
[110] Heiner C E, Dreyer J, Hertel I V, Koch N, Ritze H H, Widdra W and Winter B 2005 *Appl. Phys. Lett.* **87** 093501

[111] Koch N, Pop D, Weber R L, Böwering N, Winter B, Wick M, Leising G, Hertel I V and Braun W 2001 *Thin Solid Films* **391** 81
[112] Ishii H, Hayashi N, Ito E, Washizu Y, Sugi K, Kimura Y, Niwano M, Ouchi Y and Seki K 2004 *Phys. Status Solidi* a **201** 1075
[113] Gavrila G N, Mendez H, Kampen T U, Zahn D R T, Vyalikh D V and Braun W 2004 *Appl. Phys. Lett.* **85** 4657
[114] Hasegawa S, Mori T, Imaeda K, Tanaka S, Yamashita Y, Inokuchi H, Fujimoto H, Seki K and Ueno N 1994 *J. Chem. Phys.* **100** 6969
[115] Koch N, Vollmer A, Salzmann I, Nickel B, Weiss H and Rabe J P 2006 *Phys. Rev. Lett.* **96** 156803
[116] Yamane H, Kera S, Okudaira K K, Yoshimura D, Seki K and Ueno N 2003 *Phys. Rev.* B **68** 033102
[117] Koller G, Berkebile S, Oehzelt M, Puschnig P, Ambrosch-Draxl C, Netzer F P and Ramsey M G 2007 *Science* **317** 351
[118] Koch N, Zojer E, Rajagopal A, Ghijsen J, Johnson R L, Leising G and Pireaux J J 2001 *Adv. Funct. Mater.* **11** 51
[119] Koch N, Chan C, Schwartz J and Kahn A 2003 *Phys. Rev.* B **67** 195330
[120] Koch N, Jäckel F, Ghijsen J, Rojas M C, Grioni M, Rabe J P, Johnson R L, Kahn A and Pireaux J-J 2005 *J. Electron Spectrosc. Relat. Phenom.* **144–147** 495